ADVANCING EARTH AND SPACE SCIENCES

GeoHealth

RESEARCH ARTICLE

10.1029/2025GH001654

Key Points:

- The 12 km resolution captures disparity patterns but systematically underestimates exposure levels compared with the 1 km simulation
- Electric vehicle adoption reduces summertime air pollution exposure for all groups, but exposure disparities persist across racial/ethnic populations
- Exposure reductions are greatest for minorities, with the largest benefits for Asian, followed by Hispanic and Black populations

Supporting Information:

Supporting Information may be found in the online version of this article.

Correspondence to:

J. Kaiser,
jennifer.kaiser@ce.gatech.edu

Citation:

Zhou, Y., He, X., Skipper, T. N., Li, Z., Gao, Z., Russell, A. G., & Kaiser, J. (2026). Can electric vehicles reduce summertime air pollution exposure inequalities in metro Atlanta? a high-resolution analysis. *GeoHealth*, *10*, e2025GH001654. https://doi.org/10.1029/2025GH001654

Received 10 OCT 2025
Accepted 26 AUG 2026

Author Contributions:

Conceptualization: Jennifer Kaiser
Formal analysis: Yakun Zhou, Xin He, Jennifer Kaiser
Funding acquisition: Jennifer Kaiser
Investigation: Yakun Zhou, Xin He, Jennifer Kaiser
Methodology: Yakun Zhou, Jennifer Kaiser
Supervision: Jennifer Kaiser
Visualization: Yakun Zhou, Xin He
Writing – original draft: Yakun Zhou, Xin He

Can Electric Vehicles Reduce Summertime Air Pollution Exposure Inequalities in Metro Atlanta? A High-Resolution Analysis

Yakun Zhou[1], Xin He[1], T. Nash Skipper[1], Zongrun Li[1,2], Ziqi Gao[1,3], Armistead G. Russell[1], and Jennifer Kaiser[1,4]

[1]School of Civil and Environmental Engineering, Georgia Institute of Technology, Atlanta, GA, USA, [2]Now at Department of Mechanical Engineering, Colorado State University, Fort Collins, CO, USA, [3]Now at Environmental Institute, University of Virginia, Charlottesville, VA, USA, [4]School of Earth and Atmospheric Sciences, Georgia Institute of Technology, Atlanta, GA, USA

Abstract Electric vehicles (EVs) are widely expected to improve air quality by reducing on-road emissions, but their impacts on exposure inequalities remain uncertain. To assess whether EVs can reduce summertime air pollution exposure inequalities in the Atlanta metropolitan area, we conduct high-resolution (1 km) photochemical air quality simulations using the Community Multiscale Air Quality (CMAQ) model. A 30% EV adoption of heavy-duty and light-duty vehicles is simulated to evaluate changes in nitrogen dioxide (NO_2), maximum daily 8-hr average ozone (MDA8 O_3), and fine particulate matter ($PM_{2.5}$) during summer. EV adoption leads to average domain-wide concentration reductions of 0.22 ppb in NO_2, 0.94 ppb in MDA8 O_3, and 0.06 μg/m^3 in $PM_{2.5}$, with localized increases in NO_2 and $PM_{2.5}$ near power plants from increased electricity demand. The primary driver of air quality improvement from EV adoption is the reduction in on-road vehicle emissions, which outweighs any increases in emissions from electric generating units. The largest exposure reductions are observed in communities with higher proportions of Asian, Hispanic, and Black populations, underscoring the potential for EV adoption to alleviate exposure burdens in the communities of color. However, exposure disparities persist even with EV adoption, despite overall reductions in exposure levels across all racial/ethnic groups. Coarse-resolution (12 km) simulations tend to underestimate exposure for minority groups by up to 25% for NO_2 and 10% for $PM_{2.5}$ but still capture the overall patterns of exposure disparities.

Plain Language Summary People living near busy roads or industrial areas often breathe more polluted air and face higher health risks. Electric vehicles produce no tailpipe exhaust, and a wider adoption of EVs could improve air quality. However, because EVs run on electricity, emissions can shift from roads to power plants. In this study, we use the high-resolution CMAQ model to simulate a 30% EV adoption scenario, accounting for changes in both on-road and power plant emissions. Focusing on the Atlanta metropolitan area, we find that EV adoption reduced overall pollutant levels, but the benefits are uneven: NO_2 and $PM_{2.5}$ may increase near certain power plants, while NO_2 shows localized reduction along major roadways and MDA8 O_3 exhibits more widespread reductions. The largest health gains occurred in communities with more minority residents, suggesting EVs can help reduce exposure inequalities. Coarse models missed neighborhood hot spots, highlighting the need for high-resolution modeling and cleaner electricity to maximize public health benefits.

1. Introduction

Traffic-related emissions of nitrogen oxides (NO_x; $NO_x = NO + NO_2$), volatile organic compounds (VOCs), and $PM_{2.5}$ degrade air quality and adversely affect human health. At the national scale, the transition from internal combustion engine vehicles to EVs is anticipated to improve urban air quality by reducing on-road emissions (Bistline et al., 2022; Nopmongcol et al., 2017). These benefits are likely to be most pronounced for near-road communities, which are disproportionately composed of historically disadvantaged populations (Antonczak et al., 2023; Rowangould, 2013). However, the net benefit of EV adoption and its impacts on exposure inequities are likely to vary significantly across metropolitan areas because of differences in transportation networks, urban development patterns, energy grid composition, and atmospheric chemical regimes.

Atlanta presents a critical case study for examining these potential benefits. It remains one of the most racially segregated metropolitan areas in the United States (OBI, 2025), with minority populations experiencing

Writing – review & editing:
T. Nash Skipper, Zongrun Li, Ziqi Gao, Armistead G. Russell, Jennifer Kaiser

significantly higher exposure to NO_x and $PM_{2.5}$, alongside a higher prevalence of cardiovascular and respiratory diseases (Servadio et al., 2019). Wang et al. (2023) found that minority groups in the Atlanta MSA are subjected to twice the NO_2 exposure of the low-income White population and 20% more than the high-income White population. These racial and ethnic disparities grew between 2000 and 2016 despite an overall decrease in on-road emissions, consistent with evidence that emission reductions may not reduce exposure disparities when emission reductions and air-quality improvements are spatially uneven (Koolik et al., 2024, 2025; Polonik et al., 2023). Racial segregation has contributed to unequal ambient air pollution burdens across racial groups. Predominantly minority communities are more likely to be located near hazardous sites and major emission sources (Jones et al., 2014), highlighting that localized sources remain a dominant concern. In Atlanta, the Hartsfield-Jackson International Airport represents a major contributor to local NO_2 and $PM_{2.5}$ levels (Lawal et al., 2022). However, it remains unclear to what extent EV adoption will mitigate longstanding exposure inequalities in Atlanta.

The net environmental impact of EVs is complicated by the shift of emissions from tailpipe exhaust to Electric Generating Units (EGUs) (Efstathiou et al., 2024; Hennessy et al., 2024; Holland et al., 2019; Visa et al., 2023). This is particularly important in Georgia, where EV adoption can shift emissions from tailpipes to a mix of coal-, natural gas-, or nuclear-powered generation, with ∼15%, ∼45%, and ∼27% of statewide energy production, respectively (US EIA, 2023). In the Atlanta MSA, EGU emissions and on-road sources contribute comparably to the annual mean $PM_{2.5}$ design value (Hu et al., 2022). This suggests that while EVs may reduce on-road $PM_{2.5}$ emissions, these gains could be offset by increased primary and secondary particulate matter near generating facilities. For ozone, on-road emissions of NO_x dominate, contributing approximately six times more than power generation (Hu et al., 2022), indicating a clearer potential benefit from electrification.

Previous national-scale studies provide a useful estimate of the total air quality improvements expected from EV adoption (Hennessy et al., 2024; Nopmongcol et al., 2017; Peters et al., 2020; Schnell et al., 2019; Tessum et al., 2014). For example, Bistline et al. (2022) estimate that modeled ozone design values in the Southeastern United States are reduced by 12 ppb under limited electrification scenarios. Pan et al. (2023) find that aggressive EV uptake would prevent 180 premature air pollution related deaths annually and yield economic benefits of $1.96 billion in the Atlanta metropolitan area, based on simulations at a coarse 12 km resolution. These and other studies are often performed using chemistry-transport models with a spatial resolution of typically 12 km or coarser, which is insufficient for capturing the steep spatial gradients of short-lived primary pollutants like NO_2. Assessing environmental inequities requires higher-resolution simulations capable of resolving near-road gradients and intra-urban variability. Fine-scale assessments for other cities such as Chicago, Houston, and Los Angeles have been conducted (Camilleri et al., 2023; Li et al., 2024; Pan et al., 2019); however, no neighborhood-scale analysis has been performed for Atlanta. With Georgia ranking eighth nationally in EV registrations in 2023 (US DOE, 2023), a high-resolution analysis for Atlanta offers a valuable opportunity to examine the future implications of continued EV adoption for air quality and exposure disparities.

We selected summertime to study exposure disparities because it represents the most photochemically active period with high ozone pollution. In 2017, more than half (56%) of days with MDA8 O_3 exceeding 70 ppb in the Atlanta MSA occurred during the summer months (June–August). In addition, multiple studies have shown that summer seasons are associated with elevated health risks (Lüthi et al., 2023; Shindell et al., 2024). For example, in Atlanta, a summer temperature of 32°C is associated with a 5%–15% increase in the risk of premature mortality relative to the minimum level (Weinberger et al., 2017).

Here, we employ the Community Multiscale Air Quality (CMAQ) model at 1 km resolution to investigate the impact of EV adoption on summertime NO_2, MDA8 O_3, and $PM_{2.5}$ concentrations in the Atlanta metropolitan area, Georgia, USA. Our focus on summertime is motivated by higher ozone production rates and steeper NO_2 spatial gradients. We simulate a 30% EV adoption scenario, using a power dispatch model to estimate additional emissions from EGUs, and compare it with the noEV scenario at both 12 and 1 km resolutions to quantify the air quality changes. We diagnose the effect of spatial resolution on exposure disparities and burden of air pollution between racial/ethnic populations in the Atlanta MSA, comparing results from 1 to 12 km resolutions. Specifically, we assess how high-resolution simulations influence estimates of racial/ethnic exposure disparities.

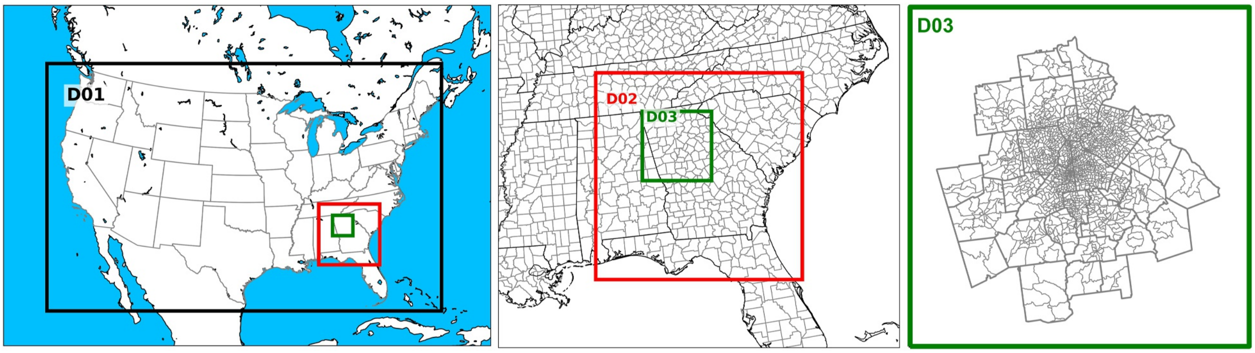

Figure 1. Nested spatial domains used in this study: the 12 km domain (d01, black box) covers the contiguous United States, the 4 km domain (d02, red box) covers Georgia and surrounding states, and the 1 km domain (d03, green box) is the study domain. The rightmost panel shows the Atlanta MSA at the census tract level within the d03 1 km domain.

2. Methods

2.1. CMAQ Simulation

We conduct air quality simulations for July 2017 using the CMAQ model version 5.4 with the CB6r3 chemical mechanism (US EPA, 2022a). We use three nested domains with resolutions of 12, 4, and 1 km (Figure 1). The 12 km domain is driven by hemispheric CMAQ (HCMAQ) (Mathur et al., 2017) to provide initial and boundary conditions. For 4 and 1 km simulations, initial and boundary conditions are provided by the corresponding parent domains. In this study, we focus on comparing 12 and 1 km model resolutions to examine how spatial resolution affects exposure assessment. Therefore, the 4 km simulation is not discussed further in the results and analysis. To minimize the influence of initial conditions, we use a spin-up time of 10 days (June 21–30, 2017).

Meteorological data are provided by the Weather Research and Forecasting (WRF) Model, version 4.4 (Skamarock et al., 2019), using the North American Mesoscale (NAM) Analysis and observational data sets for nudging WRF toward observations. WRF Model simulations use the same grid definitions as CMAQ (Figure 1). The 12 km resolution NAM (NCAR, 2015) data provided the initial and boundary conditions. We utilize grid nudging and observational nudging with the NCEP ADP global surface (NCAR, 2004a) and upper air observational weather data (NCAR, 2004b) to improve the model performance. The Meteorology-Chemistry Interface Processor (Byun et al., 1999; Otte & Pleim, 2010) is applied to WRF outputs to provide the meteorological input files required for CMAQ. WRF nudging coefficients are shown in Table S1 in Supporting Information S1, and WRF model performance is evaluated in Section 3.1.

In the base scenario, emissions are derived from the 2017 emissions modeling platform developed by the U.S. Environmental Protection Agency (US EPA, 2022b) based on the 2017 National Emissions Inventory (NEI) (US EPA, 2021). In the 1 km simulation, on-road emissions are replaced with high-resolution emissions from the Neighborhood Emission Mapping Operation (NEMO), which is produced at hourly intervals based on the 2017 NEI (Ma & Tong, 2022b). The base scenario is used to evaluate CMAQ model performance, as discussed in Section 3.1.

We examine two additional model scenarios: a scenario with current energy demands redistributed according to an electricity dispatch model (noEV) and a scenario in which 30% of heavy-duty and light-duty vehicles (LDVs) in the study domain are replaced with EVs (30EV). This 30% EV adoption rate aligns with the intermediate phase of the decarbonization transition (Camilleri et al., 2023), during which fossil fuel-powered EGUs are likely to provide a substantial fraction of the additional electricity demand (Grubert & Hastings-Simon, 2022). Changes in emissions from EGUs and on-road sources under these scenarios are described in the following section and summarized in Table 1.

2.2. Dispatch Model and Emissions Scenarios

In order to simulate the additional emissions from EGUs that result from increased energy demand, we use an energy emissions dispatch model, based on Deetjen and Azevedo (2019) and further applied to the Atlanta area in

Table 1
Description of Community Multiscale Air Quality Simulations

Scenario	Resolution (km)	On-road emissions	EGU emissions	
Base	1	NEMO	CEMS	
	12	NEI		
noEV	1	NEMO	Dispatch model	Baseline electricity demand
	12	NEI		
30EV	1	70% × NEMO		Additional EV electricity demand
	12	70% × NEI		

Mei et al. (2024). Details of the dispatch model are presented in Text S1 in Supporting Information S1. Briefly, EGUs in the CMAQ modeling domain are dispatched on an hourly basis according to a ranked generation cost order with additional constraints on minimum unit downtime. While electricity demand for Atlanta is supplied from an unknown distribution of facilities within the broader Southern Company (SOCO) balancing authority area, and while some electricity may also be imported from outside the SOCO balancing authority area, we note that our study domain includes several of the largest power plants in the region. Our assumption that power must come from within the domain represents a worst-case scenario for EGU emission increases from EV charging. Implications of this assumption are discussed further in Section 3.2.

The emissions from each EGU are calculated using the dispatched demand (MWh) and unit-level emission factors (kg/MWh). For NO_x and SO_2, hourly emission factors are calculated using the median weekly data in July 2017 from the EPA Continuous Emission Monitoring System (CEMS) data set (US EPA, 2023b). NO_x is apportioned to NO and NO_2 using ratios from the 2017 EPA emissions modeling platform (US EPA, 2022b). Due to the unavailability of hourly $PM_{2.5}$ data, unit-level annual emission factors were estimated using the annual $PM_{2.5}$ emissions and generation from the U.S. EPA's 2022 eGRID data set (US EPA, 2024). Total $PM_{2.5}$ mass is distributed to individual CMAQ species using ratios from the 2017 EPA emissions modeling platform (US EPA, 2022b).

To assess the skill of our dispatch model and associated emissions estimates, we first compare the results of air quality simulations using the dispatch model-derived emissions and emissions from the CEMS data set (US EPA, 2023b). In the noEV scenario, we use baseline electricity demand from the CEMS data set and distribute it to EGUs according to our dispatch model. Results of the air quality simulations for the base and noEV scenarios are discussed in Section 3.1.

We then use the dispatch model to calculate additional EGU emissions in the 30EV scenario. The additional electricity demand is calculated using Equation 1:

$$\text{extraLoad} = \sum_{k=1}^{n} \left(0.3 \cdot \text{VMT}_k \cdot \text{CE}_k \cdot (1 - \text{GTL})^{-1}\right) \tag{1}$$

where k denotes vehicle type and differentiates light-duty vehicles (LDVs) and heavy-duty vehicles (HDVs), vehicle miles traveled (VMT) are historical data for July 2017 sourced from MOVES, CE (EV charging efficiency) is assumed to be 0.275 kWh/mile for LDVs (Choma et al., 2020) and is further categorized for HDVs (Camilleri et al., 2023), and the GTL (grid transmission loss rate) is assumed to be 0.051 (Camilleri et al., 2023). Monthly extra electricity demand from Equation 1 is apportioned hourly using the hourly EV charging profiles in the Avoided Emissions and geneRation Tool (US EPA, 2023a). Diurnal cycles of charging profiles for LDVs and HDVs on weekdays and weekends are shown in Figure S1 in Supporting Information S1, and the total additional demand on electricity is shown in Figure S2 in Supporting Information S1.

For the 30EV scenario, we assume that 30% of VMT previously traveled by conventional vehicles within the study domain are traveled by EVs. Accordingly, on-road emissions in both the 1 km NEMO and the 12 km 2017 NEI are reduced by 30% across the study domain to represent the 30% EV adoption scenario. On-road emissions include both exhaust and non-exhaust emissions. In reality, EV adoption would primarily reduce exhaust emissions, while non-exhaust emissions (e.g., tire and brake wear) would remain (Timmers & Achten, 2016). In the base simulation, exhaust emissions constitute a large portion (81%) of the total on-road PM emissions, and the remaining non-exhaust emissions are brake wear (13%) and tire wear (6%). If only exhaust emissions were reduced, the expected decrease in on-road PM emissions due to 30% EV adoption would be 24% (0.3 × 81%). If EVs create additional non-exhaust emissions compared to their non-EV counterparts, then the modeled reduction may be less than 24%. Therefore, our simulation may overestimate the benefits of EVs on PM.

Because our study aims to examine the impact of model resolution on the estimated impacts of EV adoption, we construct our 12 km model simulations to achieve emissions changes similar to those in the 1 km resolution. Although the 12 km resolution domain covers a larger geographic area (d01 in Figure 1), we apply the 30% replacement of conventional vehicles only within the geographic area corresponding to the 1 km study domain, keeping on-road emissions unchanged outside the 1 km domain. Consistent with this assumption, the additional electricity demand from EV adoption is allocated to the same EGUs as in the 1 km simulation. We compare total on-road emissions between the 12 and 1 km simulations over the study domain (d03 in Figure 1). Total on-road NO_x and PM emissions are broadly consistent between the two simulations, differing by 4%, because NEMO is based on the same underlying data as the NEI.

2.3. Exposure Assessment

Our exposure analysis covers the Atlanta-Sandy Springs-Alpharetta metropolitan statistical area, referred to as the Atlanta MSA hereafter. The Atlanta MSA comprises 29 counties, 1,500 census tracts, and a total population of 6,026,734. The 2017 American Community Survey data (Manson et al., 2023) provides the demographic composition of the area, which consists of 45% non-Hispanic White, 34% non-Hispanic Black, 11% Hispanic or Latino, and 6% non-Hispanic Asian residents, with non-Hispanic Blacks concentrated near the urban core and non-Hispanic Whites more heavily represented in the suburban areas.

We calculate mean population-weighted exposure using daily concentrations of $PM_{2.5}$, NO_2, and MDA8 O_3 for different racial/ethnic groups at 1 and 12 km resolution for the Atlanta MSA using Equation 2:

$$C_{\mathrm{pop}} = \frac{\sum_i (P_i \cdot C_i)}{\sum_i P_i} \tag{2}$$

where C_{pop} is the population-weighted concentration, P_i is the population of a racial group in grid cell i, and C_i is the daily pollutant concentration in grid cell i at 1 and 12 km resolution. We use gridded population density data (people/km^2) (WorldPop, 2020) and assign them to 1 km grid cells. Population counts for the 12 km grid cells are calculated by summing the gridded population within each 12 km grid cell. Census tract level population counts are allocated to 1 km × 1 km grid cells proportionally based on the fraction of each grid cell's area relative to the total area of the corresponding census tract. Racial and ethnic population estimates at 1 km resolution are then calculated by multiplying the racial/ethnic fractions at the census tract level by the population assigned to each grid cell. Using this approach, we estimate the spatial distribution and population-weighted exposure risk for each pollutant across all racial/ethnic groups in the Atlanta MSA.

3. Results and Discussion

3.1. Model Performance Evaluation

We evaluate the performance of the base scenario CMAQ simulations for 24-hr average $PM_{2.5}$ and NO_2, and MDA8 O_3 concentrations, along with WRF-simulated temperature, relative humidity, and wind speed. Model outputs from both the 1 and 12 km simulations are compared with observational data from the U.S. EPA Air Quality System (AQS) database (US EPA, 2026). Model performance is assessed based on the mean bias and the Pearson correlation coefficient (r). Detailed information on monitoring sites is listed in Table S2 in Supporting Information S1. Modeled meteorological variables show good agreement with observations and capture observed diurnal patterns (Figure S3; Table S4 in Supporting Information S1). Model performance at the 1 and 12 km resolutions is evaluated against surface monitoring observations across the study domain and summarized in Table S5 in Supporting Information S1. For each species, the model generally reproduces daily variability during

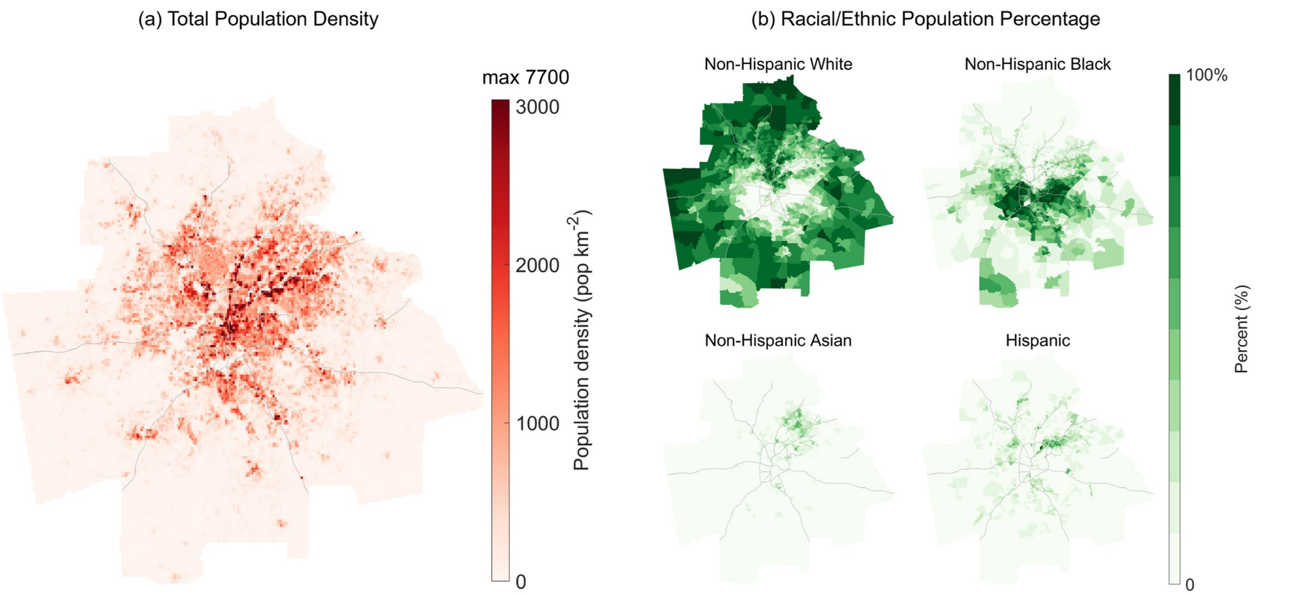

Figure 2. Spatial distribution of total population density (pop/km^2) in (a), and the percentage (%) of the total population by race/ethnicity at the census tract level across the Atlanta MSA in (b).

the study period. Overall, model performance indicates that the CMAQ simulations are suitable for evaluating summertime air quality in Atlanta and further assessing the impacts of EV adoption on pollutant concentrations.

To evaluate the influence of the dispatch model, we compare air quality simulations driven by the dispatch model with those using power plant emissions from the EPA CEMS data set. The noEV (dispatch-model-driven) simulations show strong agreement with the base scenario (CEMS-driven) results, with daily average NO_2 and $PM_{2.5}$ concentrations and MDA8 O_3 concentrations in good agreement and correlation coefficients near 1. This agreement indicates that the dispatch model can reasonably represent emission changes under EV adoption scenarios. Because the noEV simulation reflects emissions consistent with observed conditions, we use it as the baseline for population exposure. In the following analysis, pollutant concentrations in the noEV scenario represent pre-EV conditions, and the difference (noEV − EV) is used to quantify changes in air quality attributable to 30% EV adoption.

3.2. Emission Changes From On-Road and EGUs

Under the 30EV scenario, the largest on-road emission reductions occur within densely populated areas near the urban core. Total monthly average on-road NO_x emissions decrease by 1,769 kg/hr (Figure 3), and on-road $PM_{2.5}$ emissions decrease by 84 kg/hr (Figure S4 in Supporting Information S1). In contrast, increases in emissions from EGUs are spatially limited to grid cells containing power plants. EGUs located within the study domain are predominantly gas-fired units, although several large coal-fired power plants remain important contributors to emissions (Table S3 in Supporting Information S1) (US EPA, 2024). EGU NO_x emissions increase by an average of 27 kg/hr across all power plant units (Table S6 in Supporting Information S1), corresponding to a total increase of 412 kg/hr. EGU $PM_{2.5}$ emissions increase by 56 kg/hr. Coal-fired power plants account for 66% and 63% of the total increase in EGU NO_x and $PM_{2.5}$ emissions, respectively. SO_2 emissions also increase by 495 kg/hr (Table S6 in Supporting Information S1), primarily from coal combustion, and are concentrated at three coal-fired units: Bowen, Scherer, and Wansley (annotated in Figure 3). Coal-fired units account for 99.7% of the increased SO_2 emission and have baseline NO_x emission rates 5.6 times those of gas-fired facilities, such as Jack McDonough (annotated in Figure 3). Overall, reductions in on-road NO_x emissions are 4.3 times the increase in EGU NO_x emissions, and reductions in on-road $PM_{2.5}$ emissions are 1.5 times the increase in EGU emissions, resulting in a net domain-wide decrease in both NO_x and $PM_{2.5}$ emissions. Our results show that net domain-wide reductions in NO_x and $PM_{2.5}$ emissions under EV adoption are consistent with previous studies (Camilleri et al., 2023; Nopmongcol et al., 2017; Pan et al., 2019). Even after accounting for additional EGU emissions due to increased electricity demand, reductions in on-road tailpipe emissions improve air quality.

10.1029/2025GH001654

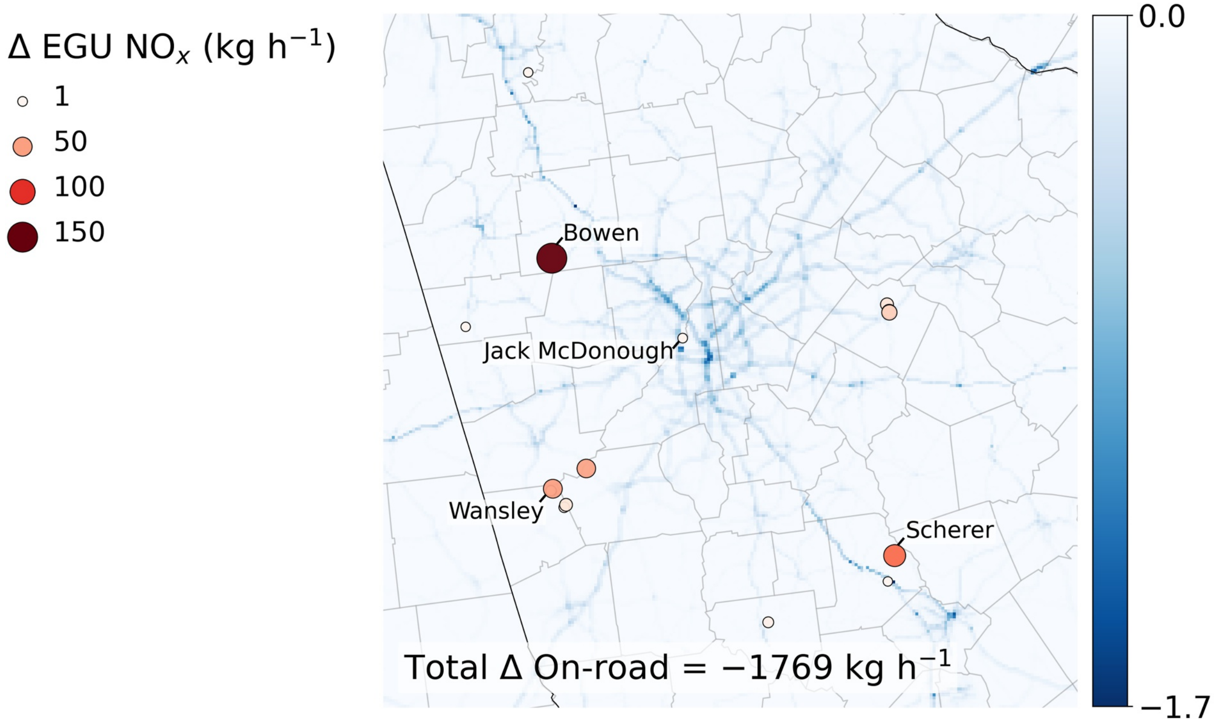

Figure 3. Spatial distribution of the monthly average decrease in on-road NO_x emission under the 30% electric vehicle adoption scenario, calculated as 30 EV − noEV. Overlaid circles indicate the monthly average increase in Electric Generating Unit NO_x emissions at individual power plant locations.

In reality, electricity demand in the Atlanta MSA is primarily supplied within the broader SOCO balancing authority area, which spans a much larger geographic region, and may also include imports from outside the SOCO balancing authority area. Based on data from the U.S. Energy Information Administration (US EIA, 2023), power plants within our study domain account for only 13% of total net electricity generation within the SOCO balancing authority area, indicating that most electricity supplied to Atlanta is generated outside the study domain. Therefore, the EGU emission changes reported here are likely to represent the worst estimate. Future grid modifications and modernization, including the retirement of coal-fired steam units, upgrades to gas combustion turbines, and the expansion of clean energy technologies, are expected to reduce emissions.

3.3. EV Impact on Air Quality

The fine-resolution simulation enables detailed characterization of spatial changes in pollutant concentrations near major roadways and power plants from EV adoption (Figure 4). In the noEV scenario, NO_2 concentrations are highest along major roads, with a domain-wide average of 1.5 ppb. MDA8 O_3 concentrations are elevated in the northeastern portion of the domain, with a domain-wide average concentration of 46 ppb, while $PM_{2.5}$ levels are concentrated near major roadways and point sources, averaging 6.2 μg/m^3 across the domain. Following a 30% EV adoption, the domain-wide average NO_2 concentration decreases by 0.22 ppb (15%), with the largest reductions occurring along roadways, though localized increases are also observed around certain power plants due to enhanced EGU emissions (black crosses in Figure 4d). MDA8 O_3 concentrations decrease 0.9 ppb (2%) on average, with widespread reductions across the study domain (Figure 4e). The largest decreases of up to 2.3 ppb occur in the northeastern area, where baseline MDA8 O_3 concentrations are also elevated (Figure 4b). This spatial pattern is consistent with the prevailing southwesterly winds that transport pollutants toward the northeast (Figure S6 in Supporting Information S1). $PM_{2.5}$ concentrations decrease by 0.06 μg/m^3 on average (1%), with decreases along roads that are more spatially spread-out than NO_2 (Figure 4f). Localized increases in $PM_{2.5}$ are observed near power plants due to additional EGU emissions. The spatial pattern of concentration changes also reflects the influence of prevailing winds. Overall, the high-resolution simulation reveals widespread decreases in NO_2, MDA8 O_3, and $PM_{2.5}$ concentrations under 30% EV adoption while capturing localized pollutant hotspots near power plants driven by elevated electricity demand.

Because ozone is a secondary pollutant that responds nonlinearly to changes in on-road NO_x emissions, we further examine its modeled response. The near-roadway and widespread decrease in MDA8 O_3 in Atlanta differ from previous fine-resolution CTM studies over Houston and Chicago, which reported increases in MDA8 O_3 along high-NO_x roadways and within urban areas following vehicle electrification (Camilleri et al., 2023; Pan et al., 2019; Visa et al., 2023). In those studies, near roadways ozone increases were due to O_3 titration by NO as on-road NO_x emissions declined. At the broader urban scale, O_3 increases in these cities were favored by VOC-limited regime, under which reductions in NO_x can lead to higher ozone concentrations. Similar increases in MDA8 O_3 have been reported in coarse-resolution CTM simulations over VOC-limited regions such as Los Angeles (Skipper et al., 2023).

In our Atlanta simulation, baseline MDA8 O_3 concentrations are broadly elevated across the urban area, and lower concentrations along major roadways are shown more clearly in the zoomed-in map in Figure S7b in Supporting Information S1. For example, the MDA8 O_3 concentration at the I-20 and I-75/I-85 interchange near the center of the ring-road network is 52 ppb, compared with 55 ppb in nearby urban areas 3–5 km away. Morning maps and diurnal patterns provide evidence of near-road O_3 titration. During 06:00–09:00 LT, NO concentrations are highest and O_3 concentrations are lower over the roadway network (Figures S7 and S8 in Supporting Information S1). Reductions in NO under the 30EV scenario weaken this titration and increase morning O_3 by up to 2 ppb at the highway interchange (Figure S8d in Supporting Information S1). This early-morning O_3 increase does not produce an increase in MDA8 O_3. The daily maximum 8-hr window generally begins around 11:00–12:00 LT, after roadway NO concentrations have declined and the titration effect has weakened. At the highway interchange, hourly O_3 changes become negative after 11:00 LT (Figure S8d in Supporting Information S1). Therefore, ΔMDA8 O_3 along roadways remain slightly negative and close to zero, while larger reductions occur across the surrounding urban area (Figure 4e). The widespread negative response suggests that decreased daytime photochemical O_3 production associated with lower NO_x emissions dominates the MDA8 O_3 response across the Atlanta domain. Our simulation is consistent with previous studies; the ozone production chemistry of Atlanta is primarily NO_x-limited (Cardelino & Chameides, 1995; Sillman et al., 1995). Because highly reactive biogenic VOCs are abundant in Atlanta, particularly isoprene, which contributes substantially to total VOC reactivity, ozone formation became more sensitive to NO_x (Duncan et al., 2010). Oxidation of these VOCs produces peroxy radicals that drive the conversion of NO into NO_2 and subsequently form O_3. Under these NO_x-limited conditions, NO_x availability limits photochemical ozone production, so substantial reductions in NO_x emission decrease photochemical ozone formation.

To better understand the relative contributions of on-road emission reductions and EGU emission increases to air quality, we compare their effects. While a previous source apportionment study in the Atlanta MSA reported near-equal contributions (~10%) of EGU emissions and on-road emissions to annual mean $PM_{2.5}$ design values (Hu et al., 2022), our results indicate that reductions in on-road emissions have a significantly greater impact than increases in EGU emissions under a 30% EV adoption scenario. As a result, net emissions decrease across the domain, leading to widespread improvements in air quality. Power plants are generally located in areas with lower population density, resulting in a smaller marginal population exposure per unit mass emitted (Choma et al., 2020). In contrast, tailpipe emissions occur disproportionately in large metropolitan areas where on-road emissions are concentrated along the major roadways, leading to larger marginal impacts. In addition, emissions from power plants are released from high stacks and undergo dispersion before reaching the surface, whereas tailpipe emissions are emitted directly at ground level. Under the 30EV scenario, reductions in on-road emissions drive substantial air quality improvements despite additional emissions from EGUs. Within our study domain, natural gas accounts for 82% of electricity generation, while only three coal-fired plants remain (Table S3 in Supporting Information S1). One of these coal-fired plants retired in 2023 according to EPA's 2023 eGRID database (US EPA, 2024), indicating an ongoing shift toward a lower-coal electricity generation mix. Although this retirement is not represented in our 2017 base simulation, continued grid modernization, including coal-unit retirements and upgrades to natural-gas generation, could further reduce EGU emissions in future EV-adoption scenarios. As discussed in Section 3.2, our approach allocates all additional electricity generation to EGUs within the study domain and therefore likely overestimates both the magnitude and spatial concentration of local EGU emission increases. These results should thus be interpreted as a sensitivity scenario rather than as a realistic representation of regional electricity dispatch. Previous studies have also reported net air quality benefits from EV adoption in the Atlanta MSA. For example, Holland et al. (2019) showed that urban counties in Atlanta, such as Fulton County, experience net environmental benefits from EV adoption. Bistline et al. (2022) reported larger

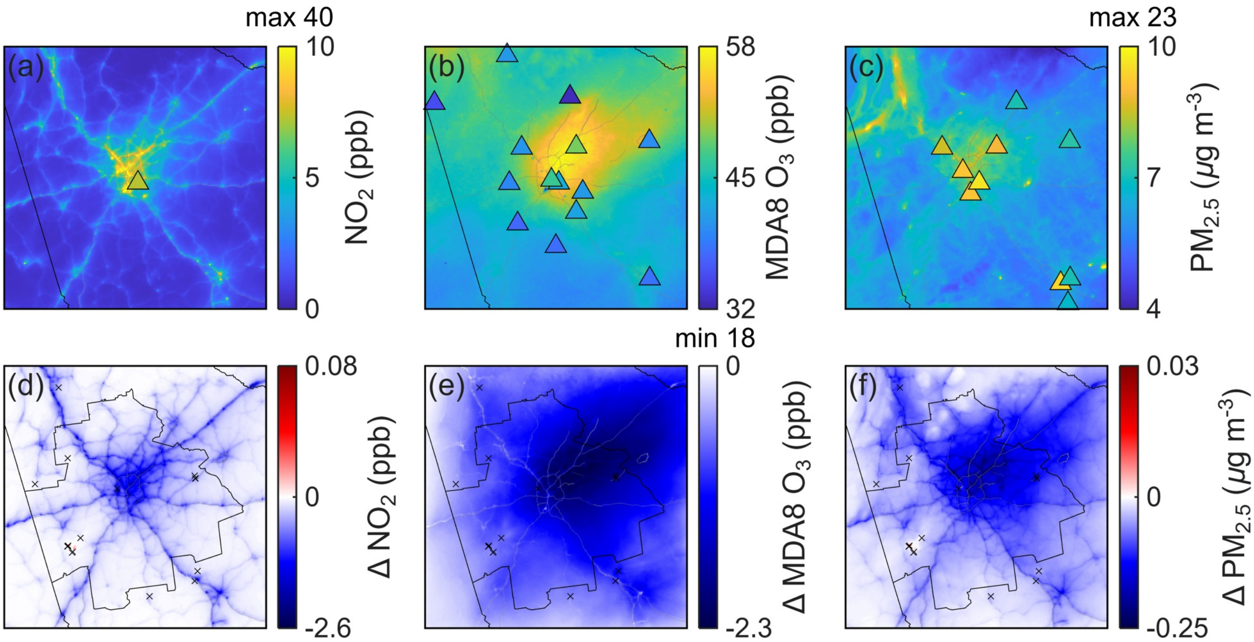

Figure 4. Spatial distribution of monthly average air pollutant concentrations for July 2017 over the study domain at 1 km resolution. Panels show (a) NO_2 (ppb), (b) MDA8 O_3 (ppb), and (c) $PM_{2.5}$ (μg/m^3). Triangle markers indicate air quality system sites used for model evaluation (Table S2 in Supporting Information S1). Major roadway networks are gray. Panels of monthly average changes in (d) NO_2 (ppb), (e) MDA8 O_3 (ppb), and (f) $PM_{2.5}$ (μg/m^3) under the 30% electric vehicle adoption scenario at 1 km resolution. Negative values indicate concentration reductions, while positive values indicate increases. Black crosses mark the locations of power plants, and the black outline denotes the boundary of the Atlanta MSA.

reductions in ozone design values (up to 12 ppb at the Fulton site) under a limited electrification scenario, primarily driven by substantial on-road NO_x emission reductions (~50%). Our study focuses on a single summer month and shows a 5 ppb decrease in the 99th percentile MDA8 O_3 under a 30% reduction in on-road NO_x emissions. The smaller reduction in our study likely reflects differences in study design, including the use of a summertime-only analysis and the absence of additional changes in off-road emissions (e.g., up to 66%) considered in previous work.

In the Atlanta region, reductions in on-road emissions outweigh increases in EGU emissions, making on-road emission reductions the primary driver of air quality improvements under current energy conditions. In Georgia, the ongoing and future energy transition away from coal-fired generation toward cleaner energy sources, including the substitution of fossil fuels, is expected to reduce upstream emissions associated with electricity generation and enhance the net benefits of vehicle electrification.

3.4. Changes in Exposure Disparities

In the noEV scenario, the highest pollutant levels for NO_2, MDA8 O_3, and $PM_{2.5}$ are observed in communities of color, particularly among Asian, Hispanic, and Black populations (Figure 5). More than 61% of communities of color are exposed to the highest NO_2 levels (Figure S9b in Supporting Information S1). Compared with White residents, NO_2 exposure is 45% higher for Asian populations, 34% higher for Hispanic populations, and 14% higher for Black populations. Similar patterns are observed for MDA8 O_3 and $PM_{2.5}$, with more than half of communities of color exposed to the highest concentrations (Figures S9d and S9f in Supporting Information S1). Asian populations experience the highest mean exposure levels for MDA8 O_3 (51 ppb) and $PM_{2.5}$ (5.4 μg/m^3), which are 7% and 10% higher than those for White populations, respectively. These patterns are consistent with previous findings in the Atlanta MSA. Wang et al. (2023) reported that Asian populations exhibit the highest mean NO_2 exposure, with levels 70% higher than those of low-income White populations and 40% higher than those of high-income White populations. The authors attributed this pattern to the concentration of first-generation Asian immigrants in densely populated urban neighborhoods near major roadways, despite the higher average education and income levels of Asian populations. In contrast, White populations in our study consistently experience the lowest exposure levels across all three pollutants (Figure 5), with a larger proportion

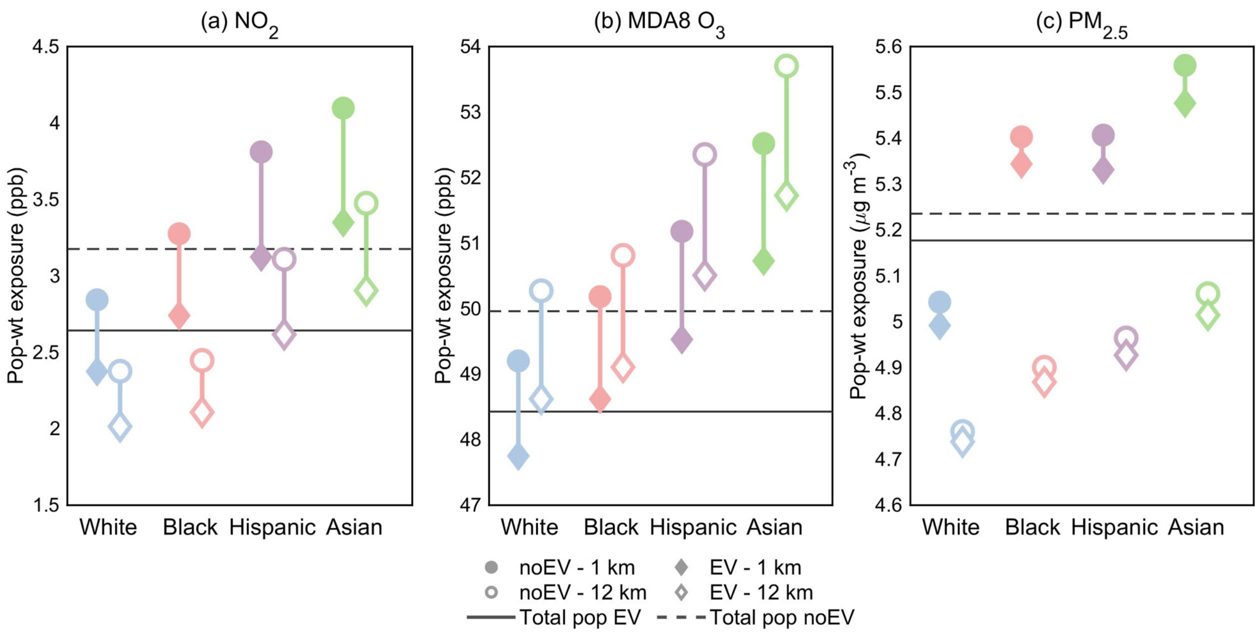

Figure 5. Population-weighted exposure for (a) NO_2, (b) MDA8 O_3, and (c) $PM_{2.5}$ across racial/ethnic groups in the Atlanta MSA under noEV and electric vehicle (EV) scenarios. Solid symbols represent 1 km resolution and open symbols represent 12 km resolution; circles denote the noEV scenario and diamonds denote the EV scenario. Horizontal lines indicate the total population-weighted exposure at 1 km resolution.

falling within the lowest NO_2 and $PM_{2.5}$ concentration deciles (Figures S9b and S9f in Supporting Information S1). Spatial distributions show that a substantial fraction of the White population resides outside the urban core (Figure 2b), in areas characterized by lower population density and traffic activity. This finding is consistent with Park and Kwan (2020), who reported that White residents in the Atlanta metropolitan area benefited from living in suburban/exurban areas farther from high-traffic roads. The authors further suggested Black and Hispanic residents more likely lack access to private vehicles, face greater mobility constraints and depend more heavily on public transit. This limited mobility, combined with racial discrimination in housing and residential segregation, may contribute to the concentration of Black and Hispanic populations in inner-city and inner-ring suburban areas with high traffic volumes.

Under the 30% EV adoption scenario, pollutant exposure levels decrease across all racial/ethnic groups for NO_2, MDA8 O_3, and $PM_{2.5}$ (Figure 5). Population-weighted concentrations for the total population are projected to decrease by 17% for NO_2 (0.6 ppb), 3% for MDA8 O_3 (1.5 ppb), and 1% for $PM_{2.5}$ (0.06 μg/m^3) based on the 1 km simulation. EV adoption reduces NO_2 exposure for all groups, with the greatest benefits occurring in communities historically experiencing higher pollution levels. People experiencing the largest exposure reductions in NO_2 and MDA8 O_3 are predominantly from minority groups (57%–59%) (Figures 6b and 6d). However, the patterns of concentration reductions differ among racial groups for short-lived NO_2 compared with more widespread MDA8 O_3 and $PM_{2.5}$. For NO_2, the decile pattern of concentration reduction reflects proximity to major roadways, where tailpipe emission reductions are most evident. NO_2 reductions are greatest for Asian residents, followed by Hispanic, Black, and White residents (Figure 6a). In contrast, reductions in MDA8 O_3 and $PM_{2.5}$ follow a different spatial pattern driven by atmospheric transport. The largest reductions occur among Asian and Hispanic populations (Figure 6c), who are more likely to reside downwind of the Atlanta urban area (Figure 2b). Black populations have the smallest reductions, as many communities are located south of the urban core and relatively upwind (Figure 2b), where decreases in MDA8 O_3 and $PM_{2.5}$ concentrations are less pronounced (Figure 4e). Residential patterns shaped by racial segregation further contribute to these differences, as communities located upwind of the urban core experience smaller air quality improvements and therefore receive fewer benefits from EV adoption. As a result, exposure reductions from EV adoption vary among racial/ethnic groups.

These findings demonstrate that EV adoption not only improves overall air quality but also provides larger benefits to minority communities. Because NO_2 is directly linked to emissions, it exhibits larger racial and ethnic exposure disparities than pollutants with substantial secondary formation, such as ozone and $PM_{2.5}$. The spatial

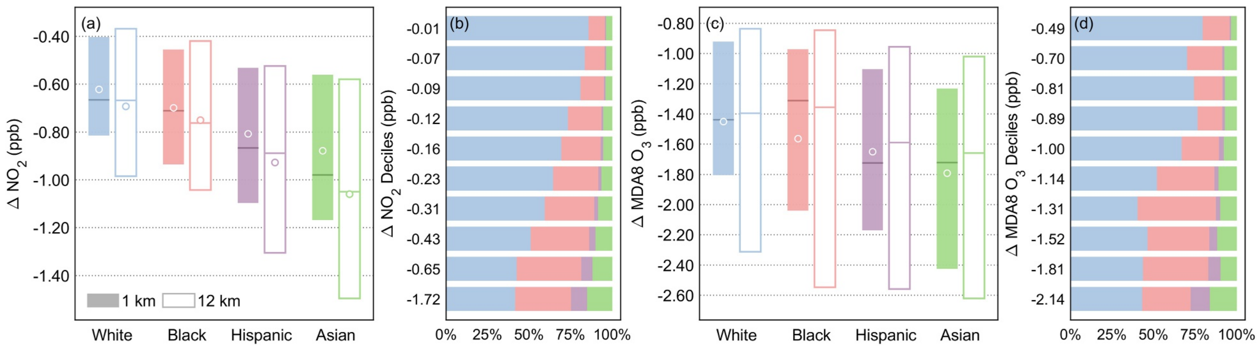

Figure 6. Monthly NO_2 and MDA8 O_3 exposure changes under the 30% electric vehicle adoption across racial/ethnic groups in the Atlanta MSA. Panels (a) and (c): distribution of changes in NO_2 and MDA8 O_3 exposures for the 1 and 12 km simulations. Circles indicate the group mean, horizontal lines indicate the group median, and vertical bars span the interquartile range (25th–75th percentile). All groups show negative mean values, indicating overall concentration reductions. Panels (b) and (d): stacked bar chart showing the exposure distribution across deciles, stratified by race/ethnicity in the 1 km simulation. Midpoints of exposure deciles are shown on the *y*-axis. Colors represent the same racial/ethnic groups across all panels.

distributions of these secondary pollutants are more strongly influenced by meteorology and atmospheric chemical regimes. As discussed in Section 3.3, summertime ozone formation in Atlanta is primarily NO_x-limited, and reductions in on-road NO_x emissions lead to widespread decreases in MDA8 O_3. Higher temperatures and abundant biogenic VOCs enhance photochemical activity, while prevailing southwesterly winds transport NO_x and other ozone precursors downwind (Figure S6 in Supporting Information S1), contributing to elevated ozone concentrations in the northeastern portion of the study domain. Exposure disparities in the Atlanta MSA have widened over time despite overall reductions in on-road emissions (Wang et al., 2023). Our results show that EV adoption reduces air pollution exposure levels for all groups. However, it does not fully eliminate exposure inequities. Communities of color remain exposed to higher-than-average pollutant levels both before and after EV adoption (Figure 5), indicating persistent disparities. Although population-weighted exposure decreases for all groups, the relative reductions are similar across racial/ethnic groups (16%–18% for NO_2, 3% for MDA8 O_3, and 1% for $PM_{2.5}$).

These persistent disparities likely reflect high traffic activity in densely populated urban core areas, where minority communities are disproportionately located. Major non-road sources of NO_x and $PM_{2.5}$, including emissions from the Atlanta airport (located near the urban center) and EGUs, also continue to impact surrounding communities as on-road emissions decline. Although the 30EV scenario reduces population-weighted exposure for all racial/ethnic groups, the similar percentage reductions across groups indicate that the relative distribution of exposure remains largely unchanged. This pattern underscores the conclusion of Koolik et al. (2025) that reducing relative disparities in vehicle-related pollution requires policies that address the disproportionate geographic concentration of emissions in overburdened communities. Polonik et al. (2023) similarly found that air-pollution disparities generally persisted under broad emission-reduction scenarios and that the largest equity improvements resulted from directly targeting emissions in communities of color, with transportation-sector reductions offering particularly strong potential to reduce racial disparities. Reducing relative exposure disparities in Atlanta may therefore require more spatially targeted measures than uniform adoption of EVs.

Overall, our results suggest that while 30% EV adoption can effectively reduce traffic-related exposure, it is insufficient to eliminate exposure disparities. Reducing persistent relative exposure disparities in Atlanta will require targeted emission reductions in overburdened communities, together with longer-term policies that address the residential segregation and transportation infrastructure.

3.5. Impact of Spatial Resolution

Fine-resolution modeling (1 km) more effectively captures sharp spatial gradients in pollutant concentrations, particularly near major emission sources. At 1 km resolution, on-road emissions are represented as highly localized along major roadway networks, resulting in higher NO_2 concentrations along roads and lower concentrations in surrounding areas. In contrast, at 12 km resolution, emissions are spatially averaged across much larger grid cells, leading to a smoothing of concentration gradients (Figures S11a and S11d in Supporting Information S1). A similar resolution dependence is evident in the MDA8 O_3 response near the major roadways. In the 1 km simulation, the small MDA8 O_3 reductions remain along the roadway network, whereas this near-road contrast is not resolved in the 12 km simulation because the O_3 response to NO_x reductions are averaged over much larger grid cells (Figure S5e in Supporting Information S1). The 1 km simulation resolves localized enhancements in NO_2 and $PM_{2.5}$ near power plants, while the 12 km simulation smooths these features and fails to capture localized concentration increases, often resulting in negative changes (Figure S12 in Supporting Information S1). For example, both the Wansley and Scherer plants show localized NO_2 increases under the 30EV scenario at 1 km resolution, whereas the corresponding 12 km results show only negative mean changes (Figures S12a and S12d in Supporting Information S1), indicating a loss of spatial detail in the coarse-resolution simulation. For EGU emissions, concentration changes due to EV-induced electricity demand are generally small for $PM_{2.5}$ and more significant for NO_2 (Figure 4 and Figure S5 in Supporting Information S1). At 1 km resolution, $PM_{2.5}$ changes remain near zero across all power plants (−0.13 to 0.04 μg/m^3), with similar small changes at 12 km. However, the 12 km simulation underestimates $PM_{2.5}$ concentrations near the coal-fired Wansley plant by 8%. In contrast, the NO_2 responses are more sensitive to resolution, with the 12 km simulation consistently underestimating NO_2 concentrations by a much larger proportion (9%–42%). These differences reflect the localized nature of emissions and the inability of coarse grids to resolve sharp concentration gradients.

Coarse-resolution (12 km) simulations systematically underestimate both total exposure and racial/ethnic exposure disparities. Compared with the 1 km simulation, the 12 km simulation systematically underestimates population-weighted concentrations in the noEV scenario and the corresponding exposure changes under the 30EV scenario, particularly for NO_2 and $PM_{2.5}$. For example, under the noEV scenario, the 12 km simulation underestimates total population exposure by ∼20% and by up to 25% for communities of color. For NO_2, underestimation ranges from 25% for Black populations to 16%–19% for Asian populations (Figure 5a). This bias results from coarse grids smoothing spatial clustering of minority populations and localized emission hotspots. However, the absolute differences remain small (generally within ∼1 ppb).

Population-weighted exposure reductions also show relatively small differences between resolutions. The 1 km simulation estimates a larger average reduction in NO_2 exposure (17%) compared with the 12 km simulation (14%), while differences are smaller for $PM_{2.5}$ (1% vs. 0.5%) and negligible for MDA8 O_3 (∼3% in both cases) (Figure 5). These smaller differences reflect the longer atmospheric lifetimes and broader spatial transport of ozone and $PM_{2.5}$ compared with NO_2. Our findings are consistent with the previous study showing that spatial resolution has a greater impact on NO_2 exposure disparities (Zalzal et al., 2024), which exhibits rapid decay with distance from emission sources, while coarse-resolution simulations tend to underestimate exposure disparities. Prior work also reported relatively small differences between 4 and 12 km resolutions for more spatially distributed pollutants, such as $PM_{2.5}$ (Paolella et al., 2018).

In summary, fine spatial resolution enables capturing pollutant enhancements near major roadways and power-plant hotspots associated with increased electricity demand. In particular, the 1 km modeling resolves the strong spatial heterogeneity of NO_2, which has a relatively short atmospheric lifetime compared with ozone and $PM_{2.5}$, potentially resulting in higher exposure disparity among racial/ethnic communities. Our results suggest that high-resolution modeling is necessary to assess neighborhood-scale exposure, especially for minority populations living near emission sources such as roadways and industrial facilities. Coarse-resolution simulations tend to underestimate exposure levels for these populations, particularly for NO_2. However, the relative differences between fine and coarse resolutions are small for all three pollutants. Coarse-resolution simulations can still capture the overall pattern of exposure disparities between groups, as they reflect broader urban–suburban gradients and population distributions. For example, a previous study has shown that the influence of spatial resolution is less pronounced in rural areas (Thompson et al., 2014). The extent to which coarse resolution represents exposure disparities may depend on the spatial distribution of populations and the degree of racial segregation in a given city.

3.6. Limitations

This study has several limitations. First, model evaluation for daily NO_2 is based on a single AQS site located within the Atlanta MSA, in a forested residential area that represents urban background conditions, so we cannot comment on the modeled representation of spatial variability across the study domain due to limited observations. Second, our study assumes non-exhaust emissions (e.g., brake and tire wear) decrease proportionally with the 30% reduction in conventional internal combustion engine vehicles. However, non-exhaust emissions may not decline proportionally with EV adoption. Regenerative braking systems can reduce brake-wear emissions for EVs relative to conventional vehicles, but tire wear, road-surface wear, and road-dust resuspension remain significant sources of non-exhaust emissions (Timmers & Achten, 2016). In addition, the generally greater weight of EVs may increase tire- and road-wear emissions (Simons, 2016). Therefore, if non-exhaust emissions decline less than assumed under future EV adoption scenarios, the exposure reduction estimated in this study could be overestimated.

4. Implications and Conclusion

To our knowledge, this is the first study to quantify exposure disparities from vehicle electrification at 1 km resolution in the Atlanta MSA. Our results show that the air-quality effects of EV adoption cannot be generalized across metropolitan areas without considering local ozone chemical regimes and the spatial resolution used to represent near-road emission gradients and chemical processes. Although Atlanta serves as a case study, similar responses may occur in other southeastern U.S. cities where abundant biogenic VOC emissions contribute to NO_x-sensitive summertime ozone formation. In these regions, communities near major roadways may benefit from reductions in both directly emitted traffic-related pollutants and photochemical ozone production following lower NO_x emissions. In Atlanta, the 30EV scenario produces the largest exposure reductions among Asian, Hispanic, and Black populations, but does not eliminate relative exposure disparities. Reducing these persistent inequities will likely require targeted emission reductions in overburdened communities, together with longer-term policies that address racial residential segregation and transportation infrastructure.

We demonstrate that a 30% adoption of EVs in the Atlanta MSA improves summertime air quality and reduces exposure levels across all groups but does not eliminate persistent exposure disparities. EV adoption leads to net emission reductions of 1,769 kg/hr for NO_x and 84 kg/hr for $PM_{2.5}$, resulting in domain-wide average concentration reductions of 0.22 ppb in NO_2, 0.94 ppb in MDA8 O_3, and 0.06 μg/m^3 in $PM_{2.5}$. The primary driver of air quality improvement from EV adoption is the reduction in on-road vehicle emissions, which outweighs any increases in emissions from EGUs. We emphasize that high-resolution (1 km) modeling captures detailed spatial variations in pollutant concentrations near emission sources, enabling more accurate assessment of exposure disparities for communities of color living near roadways and industrial facilities at the local scale. In addition, we demonstrate that coarse-resolution (12 km) modeling is capable of capturing overall exposure disparity patterns and can be useful for environmental justice assessments at the urban–suburban scale. Overall, this work suggests that integrating emissions, population exposure, and racial/ethnic inequities is critical for evaluating the impacts of EV transition strategies.

Conflict of Interest

The authors declare no conflicts of interest relevant to this study.

Availability Statement

Air quality simulations were conducted with the Community Multiscale Air Quality (CMAQ) model version 5.4, which is publicly available from EPA (US EPA, 2022a). The Neighborhood Emission Mapping Operation (NEMO), 1-km anthropogenic emission dataset is available as described by Ma and Tong (2022a). EPA monitoring data are publicly accessible via the Air Quality System (AQS) database (US EPA, 2026). Gridded population density data is available to download on publicly available websites (WorldPop, 2020). Census tract level population and demographic data (2017 American Community Survey) were obtained from the IPUMS National Historical Geographic Information System: Version 18.0 (Manson et al., 2023).

Acknowledgments

This work was supported by the Georgia Tech Strategic Energy Institute. We thank Siqi Ma and Daniel Tong for providing the 1-km anthropogenic emissions dataset.

References

Antonczak, B., Thompson, T. M., DePaola, M. W., & Rowangould, G. (2023). 2020 near-roadway population census, traffic exposure and equity in the United States. *Transportation Research Part D: Transport and Environment*, *125*, 103965. https://doi.org/10.1016/j.trd.2023.103965

Bistline, J., Blanford, G., Grant, J., Knipping, E., McCollum, D. L., Nopmongcol, U., et al. (2022). Economy-wide evaluation of CO_2 and air quality impacts of electrification in the United States. *Nature Communications*, *13*(1), 6693. https://doi.org/10.1038/s41467-022-33902-9

Byun, D. W., Pleim, J. E., Tang, R. T., & Bourgeois, A. (1999). Meteorology-chemistry interface processor (MCIP) for Models-3 Community Multiscale Air Quality (CMAQ) modeling system (EPA/600/R-99/030).

Camilleri, S. F., Montgomery, A., Visa, M. A., Schnell, J. L., Adelman, Z. E., Janssen, M., et al. (2023). Air quality, health and equity implications of electrifying heavy-duty vehicles. *Nature Sustainability*, *6*(12), 1643–1653. https://doi.org/10.1038/s41893-023-01219-0

Cardelino, C. A., & Chameides, W. L. (1995). An observation-based model for analyzing ozone precursor relationships in the urban atmosphere. *Journal of the Air & Waste Management Association*, *45*(3), 161–180. https://doi.org/10.1080/10473289.1995.10467356

Choma, E. F., Evans, J. S., Hammitt, J. K., Gómez-Ibáñez, J. A., & Spengler, J. D. (2020). Assessing the health impacts of electric vehicles through air pollution in the United States. *Environment International*, *144*, 106015. https://doi.org/10.1016/j.envint.2020.106015

Deetjen, T. A., & Azevedo, I. L. (2019). Reduced-Order dispatch model for simulating marginal emissions factors for the United States power sector. *Environmental Science & Technology*, *53*(17), 10506–10513. https://doi.org/10.1021/acs.est.9b02500

Duncan, B. N., Yoshida, Y., Olson, J. R., Sillman, S., Martin, R. V., Lamsal, L., et al. (2010). Application of OMI observations to a space-based indicator of NOx and VOC controls on surface ozone formation. *Atmospheric Environment*, *44*(18), 2213–2223. https://doi.org/10.1016/j.atmosenv.2010.03.010

Efstathiou, C. I., Arunachalam, S., Arter, C. A., & Buonocore, J. (2024). Assessing the tradeoffs in emissions, air quality and health benefits from excess power generation due to climate-related policies for the transportation sector. *Environmental Research Letters*, *19*(6), 064007. https://doi.org/10.1088/1748-9326/ad41f1

Grubert, E., & Hastings-Simon, S. (2022). Designing the mid-transition: A review of medium-term challenges for coordinated decarbonization in the United States. *WIREs Climate Change*, *13*(3), e768. https://doi.org/10.1002/wcc.768

Hennessy, E. M., Scown, C. D., & Azevedo, I. M. L. (2024). The health, climate, and equity benefits of freight truck electrification in the United States. *Environmental Research Letters*, *19*(10), 104069. https://doi.org/10.1088/1748-9326/ad75a9

Holland, S. P., Mansur, E. T., Muller, N. Z., & Yates, A. J. (2019). Distributional effects of air pollution from electric vehicle adoption. *Journal of the Association of Environmental and Resource Economists*, *6*(S1), S65–S94. https://doi.org/10.1086/701188

Hu, Y., Odman, M. T., Russell, A. G., Kumar, N., & Knipping, E. (2022). Source apportionment of ozone and fine particulate matter in the United States for 2016 and 2028. *Atmospheric Environment*, *285*, 119226. https://doi.org/10.1016/j.atmosenv.2022.119226

Jones, M. R., Diez-Roux, A. V., Hajat, A., Kershaw, K. N., O'Neill, M. S., Guallar, E., et al. (2014). Race/Ethnicity, residential segregation, and exposure to ambient air pollution: The Multi-Ethnic Study of Atherosclerosis (MESA). *American Journal of Public Health*, *104*(11), 2130–2137. https://doi.org/10.2105/ajph.2014.302135

Koolik, L. H., Alvarado, Á., Budahn, A., Plummer, L., Marshall, J. D., & Apte, J. S. (2024). $PM_{2.5}$ exposure disparities persist despite strict vehicle emissions controls in California. *Science Advances*, *10*(37), eadn8544. https://doi.org/10.1126/sciadv.adn8544

Koolik, L. H., Bullard, R. D., Min, E., Morello-Frosch, R., Patterson, R., Salgado, M., et al. (2025). Eliminating air pollution disparities requires more than emission reduction. *Proceedings of the National Academy of Sciences*, *122*(50), e2505888122. https://doi.org/10.1073/pnas.2505888122

Lawal, A. S., Russell, A. G., & Kaiser, J. (2022). Assessment of airport-related emissions and their impact on air quality in Atlanta, GA, using CMAQ and TROPOMI. *Environmental Science & Technology*, *56*(1), 98–108. https://doi.org/10.1021/acs.est.1c03388

Li, Y., Ravi, V., Heath, G., Zhang, J., Vahmani, P., Lee, S.-M., et al. (2024). Air quality and public health co-benefits of 100% renewable electricity adoption and electrification pathways in Los Angeles. *Environmental Research Letters*, *19*(3), 034015. https://doi.org/10.1088/1748-9326/ad24cc

Lüthi, S., Fairless, C., Fischer, E. M., Scovronick, N., Ben, A., Coelho, M. D. S. Z. S., et al. (2023). Rapid increase in the risk of heat-related mortality. *Nature Communications*, *14*(1), 4894. https://doi.org/10.1038/s41467-023-40599-x

Ma, S., & Tong, D. Q. (2022a). Emission data portal for NEMO [Dataset]. *Data server at George Mason University*. www.emissionnow.org

Ma, S., & Tong, D. Q. (2022b). Neighborhood Emission Mapping Operation (NEMO): A 1-km anthropogenic emission dataset in the United States. *Scientific Data*, *9*(1), 680. https://doi.org/10.1038/s41597-022-01790-9

Manson, S., Schroeder, J., Van Riper, D., Knowles, K., Kugler, T., Roberts, F., & Ruggles, S. (2023). IPUMS national historical geographic information System: Version 18.0 [Dataset]. *IPUMS*. https://doi.org/10.18128/D050.V18.0

Mathur, R., Xing, J., Gilliam, R., Sarwar, G., Hogrefe, C., Pleim, J., et al. (2017). Extending the Community Multiscale Air Quality (CMAQ) modeling system to hemispheric scales: Overview of process considerations and initial applications. *Atmospheric Chemistry and Physics*, *17*(20), 12449–12474. https://doi.org/10.5194/acp-17-12449-2017

Mei, E. J., Gao, Z., Hopke, P. K., Ebelt, S., Rich, D. Q., & Russell, A. G. (2024). Impacts of fuel prices and regulations on electricity generation emissions and urban air quality. *ACS ES&T Air*, *1*(2), 103–112. https://doi.org/10.1021/acsestair.3c00034

NCAR. (2004a). NCEP ADP global surface observational weather data, October 1999—Continuing. https://doi.org/10.5065/4F4P-E398

NCAR. (2004b). NCEP ADP global upper air observational weather data, October 1999—Continuing. https://doi.org/10.5065/39C5-Z211

NCAR. (2015). NCEP North American Mesoscale (NAM) 12 km analysis. https://doi.org/10.5065/G4RC-1N91

Nopmongcol, U., Grant, J., Knipping, E., Alexander, M., Schurhoff, R., Young, D., et al. (2017). Air quality impacts of electrifying vehicles and equipment across the United States. *Environmental Science & Technology*, *51*(5), 2830–2837. https://doi.org/10.1021/acs.est.6b04868

OBI. (2025). *Most segregated Cities in the US, 2020 - 2023*. University of California, Berkeley. Retrieved from https://belonging.berkeley.edu/most-segregated-cities-us-2020-2023

Otte, T. L., & Pleim, J. E. (2010). The Meteorology-Chemistry Interface Processor (MCIP) for the CMAQ modeling system: Updates through MCIPv3.4.1. *Geoscientific Model Development*, *3*(1), 243–256. https://doi.org/10.5194/gmd-3-243-2010

Pan, S., Roy, A., Choi, Y., Eslami, E., Thomas, S., Jiang, X., & Gao, H. O. (2019). Potential impacts of electric vehicles on air quality and health endpoints in the Greater Houston Area in 2040. *Atmospheric Environment*, *207*, 38–51. https://doi.org/10.1016/j.atmosenv.2019.03.022

Pan, S., Yu, W., Fulton, L. M., Jung, J., Choi, Y., & Gao, H. O. (2023). Impacts of the large-scale use of passenger electric vehicles on public health in 30 US. metropolitan areas. *Renewable and Sustainable Energy Reviews*, *173*, 113100. https://doi.org/10.1016/j.rser.2022.113100

Paolella, D. A., Tessum, C. W., Adams, P. J., Apte, J. S., Chambliss, S., Hill, J., et al. (2018). Effect of model spatial resolution on estimates of fine particulate matter exposure and exposure disparities in the United States. *Environmental Science and Technology Letters*, *5*(7), 436–441. https://doi.org/10.1021/acs.estlett.8b00279

Park, Y. M., & Kwan, M.-P. (2020). Understanding racial disparities in exposure to traffic-related air pollution: Considering the spatiotemporal dynamics of population distribution. *International Journal of Environmental Research and Public Health*, *17*(3), 908. https://doi.org/10.3390/ijerph17030908

Peters, D. R., Schnell, J. L., Kinney, P. L., Naik, V., & Horton, D. E. (2020). Public health and climate benefits and trade-offs of U.S. vehicle electrification. *GeoHealth*, *4*(10), e2020GH000275. https://doi.org/10.1029/2020GH000275

Polonik, P., Ricke, K., Reese, S., & Burney, J. (2023). Air quality equity in US climate policy. *Proceedings of the National Academy of Sciences*, *120*(26), e2217124120. https://doi.org/10.1073/pnas.2217124120

Rowangould, G. M. (2013). A census of the US near-roadway population: Public health and environmental justice considerations. *Transportation Research Part D: Transport and Environment*, *25*, 59–67. https://doi.org/10.1016/j.trd.2013.08.003

Schnell, J. L., Naik, V., Horowitz, L. W., Paulot, F., Ginoux, P., Zhao, M., & Horton, D. E. (2019). Air quality impacts from the electrification of light-duty passenger vehicles in the United States. *Atmospheric Environment*, *208*, 95–102. https://doi.org/10.1016/j.atmosenv.2019.04.003

Servadio, J. L., Lawal, A. S., Davis, T., Bates, J., Russell, A. G., Ramaswami, A., et al. (2019). Demographic inequities in health outcomes and air pollution exposure in the Atlanta Area and its relationship to urban infrastructure. *Journal of Urban Health*, *96*(2), 219–234. https://doi.org/10.1007/s11524-018-0318-7

Shindell, D., Hunter, R., Faluvegi, G., & Parsons, L. (2024). Premature deaths due to heat exposure: The potential effects of neighborhood-level versus city-level acclimatization within US cities. *GeoHealth*, *8*(1), e2023GH000970. https://doi.org/10.1029/2023GH000970

Sillman, S., Al-Wali, K. I., Marsik, F. J., Nowacki, P., Samson, P. J., Rodgers, M. O., et al. (1995). Photochemistry of ozone formation in Atlanta, GA-Models and measurements. *Atmospheric Environment*, *29*(21), 3055–3066. https://doi.org/10.1016/1352-2310(95)00217-M

Simons, A. (2016). Road transport: New life cycle inventories for fossil-fuelled passenger cars and non-exhaust emissions in ecoinvent v3. *International Journal of Life Cycle Assessment*, *21*(9), 1299–1313. https://doi.org/10.1007/s11367-013-0642-9

Skamarock, W. C., Klemp, J. B., Dudhia, J., Gill, D. O., Liu, Z., Berner, J., et al. (2019). A description of the advanced research WRF version 4. In *NCAR technical note ncar/tn-556+ str, 145*.

Skipper, T. N., Lawal, A. S., Hu, Y., & Russell, A. G. (2023). Air quality impacts of electric vehicle adoption in California. *Atmospheric Environment*, *294*, 119492. https://doi.org/10.1016/j.atmosenv.2022.119492

Tessum, C. W., Hill, J. D., & Marshall, J. D. (2014). Life cycle air quality impacts of conventional and alternative light-duty transportation in the United States. *Proceedings of the National Academy of Sciences*, *111*(52), 18490–18495. https://doi.org/10.1073/pnas.1406853111

Thompson, T. M., Saari, R. K., & Selin, N. E. (2014). Air quality resolution for health impact assessment: Influence of regional characteristics. *Atmospheric Chemistry and Physics*, *14*(2), 969–978. https://doi.org/10.5194/acp-14-969-2014

Timmers, V. R. J. H., & Achten, P. A. J. (2016). Non-exhaust PM emissions from electric vehicles. *Atmospheric Environment*, *134*, 10–17. https://doi.org/10.1016/j.atmosenv.2016.03.017

US DOE. (2023). Electric vehicle registrations by State. Retrieved from https://afdc.energy.gov/data/10962

US EIA. (2023). Georgia, end-use energy consumption 2023. Retrieved from https://www.eia.gov/states/GA/overview

US EPA. (2021). 2017 National Emissions Inventory (NEI) data. Retrieved from https://www.epa.gov/air-emissions-inventories/2017-national-emissions-inventory-nei-data

US EPA. (2022a). CMAQ (Version 5.4) [Software]. *Zenodo*. https://doi.org/10.5281/zenodo.7218076

US EPA. (2022b). Technical Support Document (TSD) preparation of emissions inventories for the 2017 north American emissions modeling platform.

US EPA. (2023a). Avoided Emissions and Generation Tool (AVERT) User Manual Version 4.1. Retrieved from https://www.epa.gov/avert

US EPA. (2023b). EMC: Continuous emission monitoring systems. Retrieved from https://www.epa.gov/emc/emc-continuous-emission-monitoring-systems

US EPA. (2024). *Emissions & generation resource integrated database (eGRID)*. Office of Atmospheric Protection, Clean Air and Power Division. Retrieved from https://www.epa.gov/egrid/

US EPA. (2026). Air Quality System (AQS) [Dataset]. Retrieved from https://www.epa.gov/aqs

Visa, M. A., Camilleri, S. F., Montgomery, A., Schnell, J. L., Janssen, M., Adelman, Z. E., et al. (2023). Neighborhood-scale air quality, public health, and equity implications of multi-modal vehicle electrification. *Environmental Research: Infrastructure and Sustainability*, *3*(3), 035007. https://doi.org/10.1088/2634-4505/acf60d

Wang, Y., Liu, P., Schwartz, J., Castro, E., Wang, W., Chang, H., et al. (2023). Disparities in ambient nitrogen dioxide pollution in the United States. *Proceedings of the National Academy of Sciences*, *120*(16), e2208450120. https://doi.org/10.1073/pnas.2208450120

Weinberger, K. R., Haykin, L., Eliot, M. N., Schwartz, J. D., Gasparrini, A., & Wellenius, G. A. (2017). Projected temperature-related deaths in ten large U.S. metropolitan areas under different climate change scenarios. *Environment International*, *107*, 196–204. https://doi.org/10.1016/j.envint.2017.07.006

WorldPop. (2020). The spatial distribution of population density in 2017 based on country total adjusted to match the corresponding UNPD estimate, United States [Dataset]. *WorldPop*. https://doi.org/10.5258/SOTON/WP00675

Zalzal, J., Minet, L., Brook, J., Mihele, C., Chen, H., & Hatzopoulou, M. (2024). Capturing exposure disparities with chemical transport models: Evaluating the suitability of downscaling using land use regression. *Environmental Science & Technology*, *58*(32), 14348–14360. https://doi.org/10.1021/acs.est.4c03725

References From the Supporting Information

Lew, D., Brinkman, G., Ibanez, E., Florita, A., Heaney, M., Hodge, B.-M., et al. (2013). The Western wind and solar integration Study phase 2. https://doi.org/10.2172/1220243

US, E. I. A. (2025). Form EIA-923 detailed data with previous form data (EIA-906/920) [Dataset]. https://www.eia.gov/electricity/data/eia923/